Preliminary Study of Aerodynamic Performance for Waverider-based Hypersonic Vehicles with Dorsal Mounted Engines

Yao XIAO,[1] Kai CUI,[2] Guang-li LI,[3] and Yingzhou XU,[4]
State Key Laboratory of High-Temperature Gas Dynamics, Institute of Mechanics, Chinese Academy of Sciences, Beijing 100190, China

School of Engineering Science, University of Chinese Academy of Sciences, Beijing 100049, China

To aim at improving the aerodynamic performance of hypersonic air-breathers, a family of novel waverider-based configurations, which integrate two dorsal mounted engines, is proposed. The key feature of this type of configurations is that the lower surface of the vehicle could fully preserve the characteristics of waveriders, thus it is conducive to enhancing the lift-to-drag ratio effectively. Basic waveriders of configurations are obtained by using a method that generating waverider as two parts, which are defined by the leading edge and the trailing edge respectively. The forebody of the vehicle is designed by rotating and assembling two waverider-based-surfaces, which are the front part of basic waveriders. A group of conceptual configurations with different aspect ratio is presented. Computational Fluid Dynamics is employed to evaluate the aerodynamic performance. The results demonstrate that the maximum lift-to-drag ratio of configurations is greater than 5 in viscous condition; meanwhile, the forebody could produce a good quality flowfield for the propulsion system.

Nomenclature

AoA	=	angle of attack, deg
C_A	=	axial force coefficient
C_D	=	drag force coefficient
C_L	=	lift force coefficient
C_{mg}	=	pitching moment coefficient
C_N	=	normal force coefficient
D	=	drag, N
H	=	flight height, km
L	=	lift, N
L/D	=	lift to drag ratio
L/W	=	aspect ratio
Ma	=	Mach number
P	=	static pressure, Pa
T	=	static temperature, K
X_{CP}	=	relative x position of the pressure center
β	=	shock wave angle, deg
φ	=	pre-compression surface rotation angle, deg

---

[1] Graduate Student, State Key Laboratory of High-Temperature Gas Dynamics, Institute of Mechanics.
[2] Associate Professor, State Key Laboratory of High-Temperature Gas Dynamics, Institute of Mechanics, kcui@imech.ac.cn.
[3] Graduate Student, State Key Laboratory of High-Temperature Gas Dynamics, Institute of Mechanics.
[4] Graduate Student, State Key Laboratory of High-Temperature Gas Dynamics, Institute of Mechanics.

I. Introduction

AIR-breathing hypersonic vehicles have received much attention in recent years and series of flight tests have been performed, such as the X-51A program[1]. As a demonstrator aircraft, the main purpose is to verify the performance of the propulsion system. With the further development of air-breathing hypersonic vehicles, more factors such as large payload, long cruising range and high Lift-to-drag ratio (*L/D*) should be considered. Hence, the research of configurations, which possess well aerodynamic performance, should be put on the agenda. According to the current literatures, it is known that air-breathing hypersonic vehicles can be broadly classified into following two categories base on their intended use: 1) hypersonic missile, which with long-range fast strike capability, such as the HSSW[2] (High-Speed Strike Weapon) from the United States; 2) hypersonic airplane, which requires a large lift force and the lift-to-drag ratio, such as the SR-72 airplane[3], the HCV[4] (Hypersonic Cruise Vehicle) conceptual airplane, and the HEXAFLY[5-7] (High-Speed Experimental Fly Vehicles). To meet the launch size constraints, the layout of the first category hypersonic vehicle is designed as a slender body generally. Therefore, the configuration researches in this paper just targeted at the hypersonic airplane.

It is well known that waverider[8] configurations had been deemed as the most promising shapes due to its favorable *L/D* which is high enough to break the "*L/D* barrier"[9]. Because of that the entire bow shock wave is attached to the leading edge of the waverider when flying in the design condition, so there is no flow spillage from the lower surface to the upper surface. As a result, a waverider could obtain a large *L/D* as well as a uniformly compressed flowfield for the inlet of the scramjet. Thus, the waverider-based airframe-engine integrated design had been consider as the most competitive candidate of hypersonic vehicle configurations[10-17]. In addition, to reduce the overall drag and achieve favorable conditions for propulsion system at hypersonic speeds, the engines must be highly integrated with the airframe.

According to the integrated approach between the airframe and the propulsion system, the layout of hypersonic airplane can be divided into three types of configuration: the ventral intake layout, the flanking intake layout and the dorsal intake layout. The ventral intake layout, which adopted by the United States NASP project[18], had been studied in the eighties of last century. By using a waverider as the forebody and placing scramjets beneath the vehicle, this intake layout utilized the high *L/D* performance and the well compression property of the forebody at the same time. And this approach has aroused great concern of scientists and engineers since the viscous optimized hypersonic waveriders[19] has been proposed by K.G. Bowcutt at 1987. But the ventral intake layout also has its shortcoming. By integrating the propulsion system beneath the waverider, lateral flow would be induced inevitably. The characteristics of waveriders would be contaminated consequently, that leads to the increase of the drag force and the decrease of *L/D* performance. Different from the intake layout above, the flanking intake layout would reduce this interference because of that the inlet port is set on either side of the airplane and the scramjets could be fully buried into the airframe. Thus, the lower surface of the airplane could be designed as smooth as possible, and the abdominal space of the airframe can be fully released to contain various payloads or equipment, such as the landing gear system and the bomb bay system. The FALCON HCV program[20], which proposed by United States, is using this layout. CUI and HU et al proposed a conceptual air-breathing airplane with dual waveriders forebody[21] that its maximum *L/D* is greater than 4. Nevertheless, since the lower surface of the airplane cannot be designed as an integral waverider configuration, the aerodynamic performance of the airplane is hard to achieve the optimum. Compared with those two intake layouts above, the dorsal intake layout has more potential to improve the aerodynamic performance effectively. The reason is that the engines mounted at the dorsa of the airplane makes the entire lower surface of the airplane could be designed as a complete lifting surface. On the one hand, there is a considerable internal payloads design margin; on the other hand, the optimization design space of the lower surface becomes more flexible. Because of these advantages, the dorsal intake layout was adopted by the HSGTS[22] (Hypersonic Space and Global Transportation System) which jointly proposed by the Boeing company and ASTROX company in recent years, and the HEXAFLY which proposed by Europe. Base on the published literatures, those two projects finally chose the dorsal intake layout even the other layout was used at early stages. It can be speculated that the dorsal intake layout may become the focus of the configuration researches about the next generation hypersonic airplane.

As the HEXAFLY using the Busemann inlet, the leading edge of the lower surface in the nose region is

Figure 1. A conceptual configuration of the waverider-based hypersonic vehicles with dorsal mounted engines

defined by the inlet shape, so there is a constraint on the design of the lifting surface. With the purpose of further improving the aerodynamic performance of hypersonic air-breathers, and inspired by the design principle of the HEXAFLY, a family of novel waverider-based configurations which integrating two dorsal mounted engines are presented in this paper. A conceptual configuration is shown in Fig.1. In the present study, three parts of researches are included. Firstly, based on this conception, a splicing waverider generating method is developed. Waveriders are generated from the inner and the outer part respectively by applying this method. Afterwards, the forebody of the configuration is designed by rotating and assembling two waverider-based-surfaces, which are defined by linear edges. Moreover, four simplified conceptual configurations with different aspect ratios are generated. Computational Fluid Dynamics (CFD) simulation is applied to evaluate the aerodynamic performance of all configurations which generated by our method.

II. Design Principles of the Waverider-Based Hypersonic Vehicle

A. The Splicing Waverider Generating Method

In order to obtain such conceptual configurations, the basic waveriders should meet the unique design requirement of the forebody and maintain the flexibility while designing an overall airframe. Thus the splicing waverider generating method is developed. As shown in Fig.2, based on a known flow field, the feature of the method is that a waverider is divided into the inner and the outer parts, which are defined by the leading edge and the trailing edge respectively. The generation process is as follows: 1) the shock layer and the flow field can be obtained in a given condition; 2) point A is selected at the shock layer, then the curve AB could be generated as the trailing edge of the outer part; 3) by solving the streamline equation, we can obtain the compression surface of the outer part, and the leading edge AB' can be obtain simultaneously; 4) the curve B'C is defined as the leading edge

of the inner part, so the inner compression surface can be obtained; 5) the entire upper surface remains a free-stream surface. The angle Δ is set as a monitor to describe the turning degree between the inner and the outer part.

In this paper, conical flow is chosen as the basic flow field. The shock wave angle is set as 12 deg. The free stream Mach number is 6. Considering the requirement of rotating and assembling the forebody, the inner leading edge is defined as straight line. For the purpose of providing convenience for integrating any control surfaces at the tail of configurations, the outer trailing edge is also designed as straight line. According to the generation process above, a splicing waverider can be described by three parameters, which are the relative x position of the nose point in a conical flow field, the relative length of the line in the outer trailing edge and the aspect ratio of a waverider.
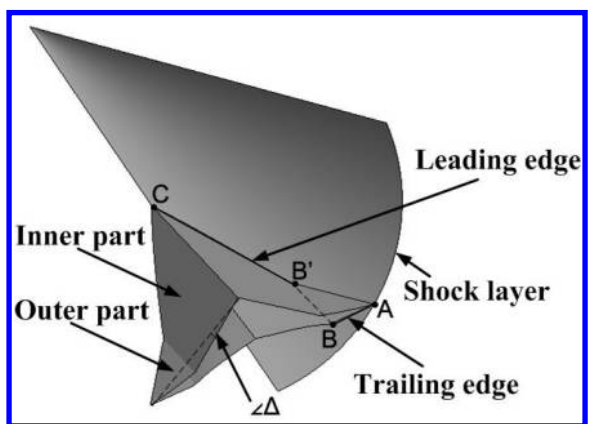

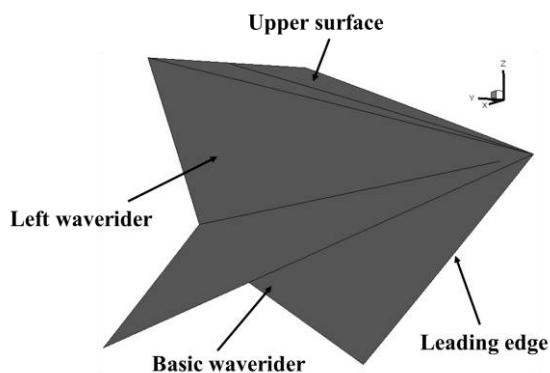**Figure 2. Sketch of a splicing waverider and definition edges**

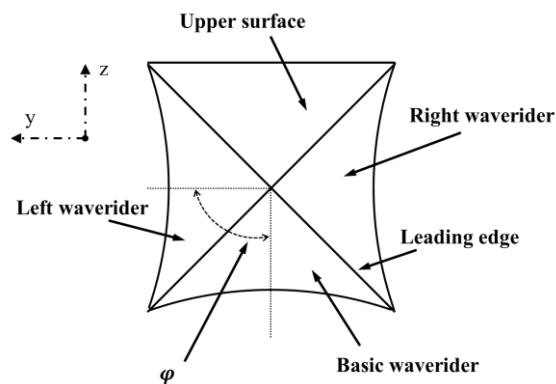**Figure 3. Three-dimensional view of the trinal waveriders forebody**

Figure 4. Sketch of a forebody (front view) and the definition of rotation angle

B. The Trinal Waveriders Forebody

Taking the waverider as the pre-compression surface can provide excellent quality flow field for the engine inlet. In addition, in consideration of the quantity of mass flow, single engine matching single waverider-based forebody will be more conducive to play the performance advantages of both. In this paper, the propulsion system assumes that two scramjet engines mounted on the dorsa of the vehicle. Thus, the forebody is designed by rotating and assembling two waverider-based-surfaces, which are the front part of basic waveriders. As a result, the forebody and the lower surface in the head region become that a layout named trinal waveriders forebody, as shown in Fig.3 and Fig.4. A brief illustration of the design procedure is as follows. First of all, the basic waverider is generated according to the method mentioned above, and its front part is cut out as the pre-compression surface. Next, the pre-compression surface is rotated along its longitudinal body axis with a predefined parameter, i.e. the rotation angle φ, which is the only parameter to describe the shape of the forebody if the length of the forebody is given. Afterwards, the rotated waverider-surface is duplicated and mirrored to generate the other pre-compression surface. Finally, the upper surface can be designed flexibly to meet the requirements of volume and aerodynamic performance. In this paper, it uses a plane surface for simplicity.

C. Preliminary Conceptual Configurations

Since the lower surface and the forebody of the vehicle are done, the airframe design is the last step to accomplish the conceptual configuration. Because of the main concern is the aerodynamic performance at this stage, the propulsion system design is not taken into account. The main design objective of the airframe is to pursue high aerodynamic performance, in particular a high L/D in small flight angle of attack, which is favorable to the operation of the forebody. Moreover, at the preliminary study stage, the simpler the shape, the better. To meet the design requirements above, a blended-wing-body layout is adopted. An example is shown in Fig.5. The control curve of the body at the cross-section is defined by a quadratic curve. The wing is design as an expansion surface, which is defined by B-spline curves.
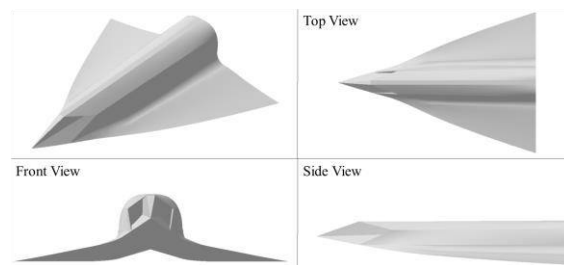

Figure 5. Three-view drawing of an example of the preliminary conceptual configurations

III.   Validation of CFD Simulation

The means to evaluate the aerodynamic performance of all configurations mentioned above is CFD simulation. The Euler equations are employed to simulate the inviscid flow and the inviscid aerodynamic performance. The implicitly coupled Reynolds-averaged Navier-Stokes (RANS) equations and the two equation k-ε turbulence model are employed to simulate the viscous flow and the viscous aerodynamic performance. The Total Variation Diminishing (TVD) difference scheme is used. With the intention of investigate the accuracy of the CFD simulation employed in this study, an experimental space shuttle case is chosen to complete the validation. The model of the space shuttle is as shown in Fig.6. The boundary conditions of the free stream are set as a Mach number of 4.96, a Reynold number per unit of 9.0×10^{6}/m, a total pressure of 1.5 MPa and a total temperature of 364 K, in accordance to the experimental setup in Ref. [23]. A structured grid, as shown in Fig.7, is adopted. In the numerical simulation process, the flight attitude of the space shuttle is set for different angles of attack, ranging from -5 deg to 25 deg, increments of 5 deg. And the angle of sideslip is set as 0.22 deg.
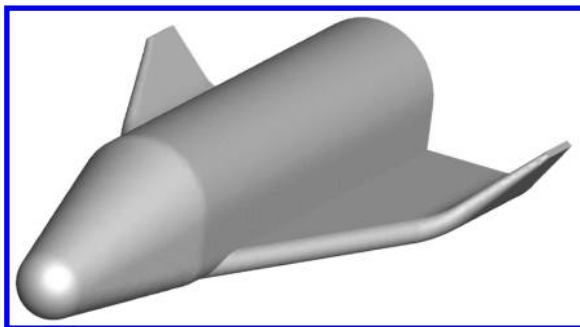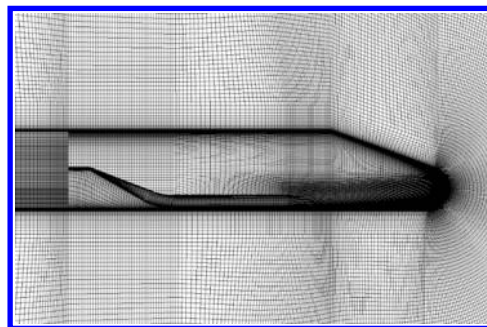

Figure 6. Model of the space shuttle

Figure 7. Structured gird of the space shuttle

4

American Institute of Aeronautics and Astronautics

The results from CFD simulation are compared with the experimental data as shown in Fig.8. It is obviously that the axial force coefficient, normal force coefficient, pitching moment coefficient and relative x position of the pressure center obtained from CFD simulation are in good agreement with the experimental data. When the angle of attack is less than 15 deg, all of the CFD data are highly consistent with the experimental data. When the angle of attack is greater than 15 deg, the force coefficients have slight deviations from the experimental data, and the deviation on pitching moment coefficient is more obvious. From this, it can be concluded that the CFD simulation in this study can evaluate the aerodynamic performance of a hypersonic vehicle within acceptable error margins, and the CFD results presented in the following section are believable.
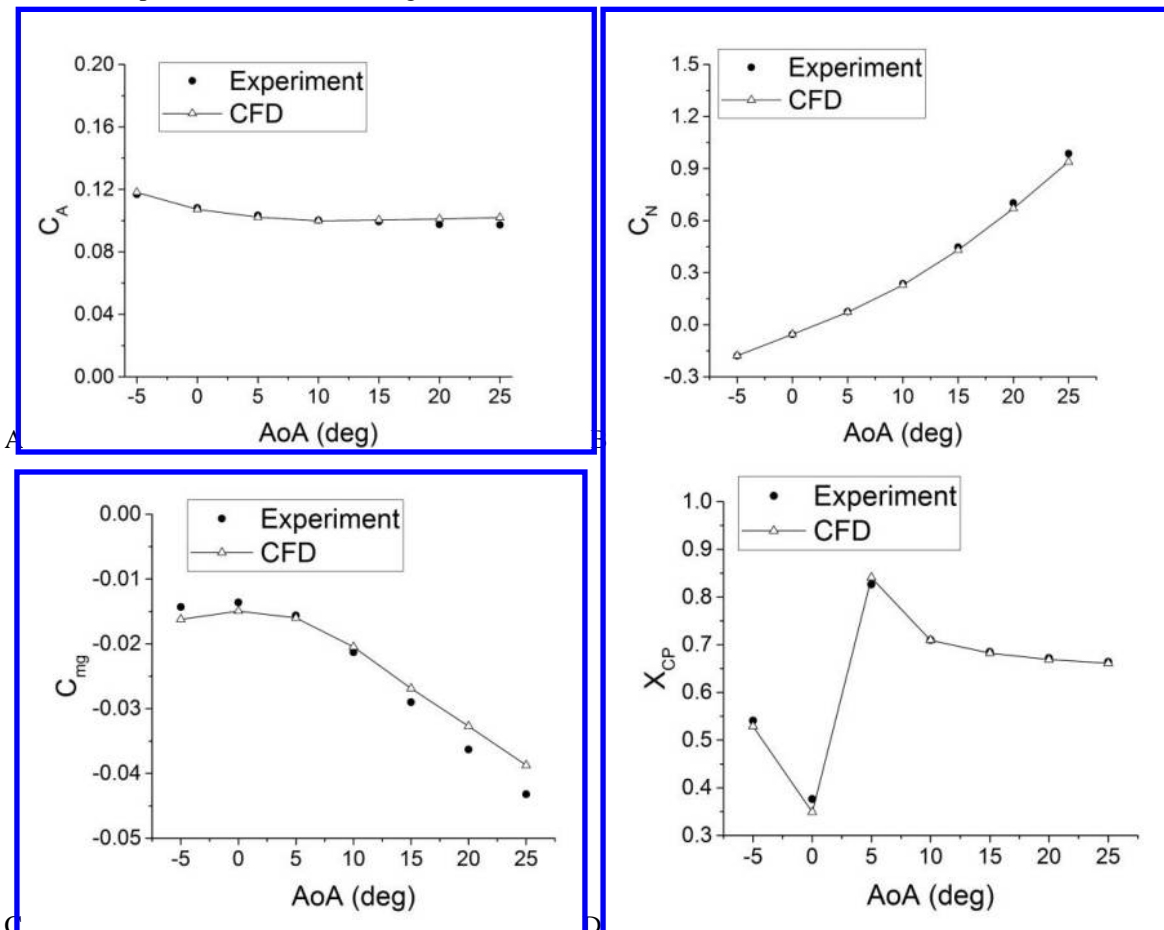

Figure 8. The space shuttle CFD simulation data compared to the experimental data. (A) Axial force coefficient. (B) Normal force coefficient. (C) Pitching moment coefficient. (D) Relative x position of the pressure center.

IV. Results and Discussions

A. Aerodynamic Performance of the Trinal Waveriders Forebody

In order to ensure that the propulsion system is located in the dorsa of the configuration, the rotation angle of the forebody should be greater than 90 deg. Besides, in order to avoid the intersection between left and right waverider-based surfaces, the rotation angle of the forebody should be less than 120 deg. To aim at figuring out the effect of rotation angle on aerodynamic performance, four forebodies with different rotation angles, which are 90deg, 100deg, 110deg and 120deg, are generated. The length of forebodies is set to 500 mm. The boundary conditions of the free stream are set as a Mach number of 6, a flight altitude of 30 km, a static pressure of 1196.983 Pa and a static temperature of 226.65 K. The angles of attack range from 0 deg to 4 deg, increments of 2 deg. The implicitly coupled RANS equations and the two equation k-ε turbulence model are employed. Structured grid is adopted, as shown in Fig.9.

The Mach number contours of four forebodies under different angle of attack are shown in Fig.10 to Fig.13. The left side of the figures is the Mach number contour line at different cross-sectional positions. The right side of the figures is the Mach number contour at the outlet cross-section. As can be seen from the figures, all of the forebodies possess the characteristic that the shock wave is attached to the leading edge of lower surface. As a result, the lower surface is fully wrapped in the high pressure behind the shock. The lower side of the forebody owns the same characteristic due to sharing the same leading edge with the lower surface. However, the shock wave is detached from the leading edge at the upper side

Figure 9. Structured gird of forebody

of the forebody because that there are lateral flow generated by the upper surface. As the rotation angle of forebody increases, the detachment of the shock wave at the upper side of the forebody becomes more obvious, except the
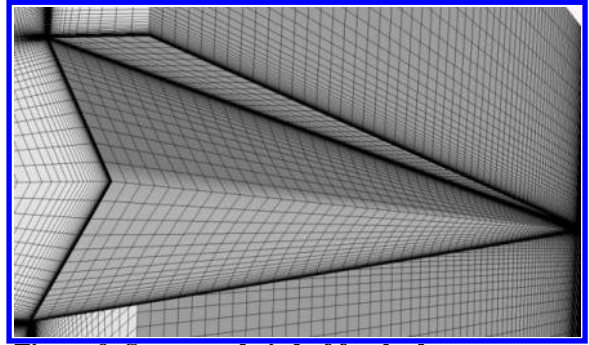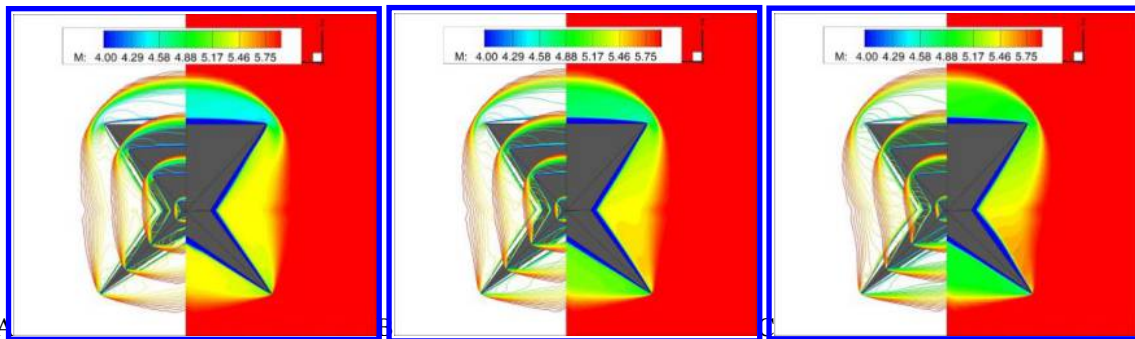

Figure 10. Mach number contours of the forebody (front view) with 90 deg rotation angle. (A) *AoA*=0 **deg. (B)** *AoA*=2 **deg. (C)** *AoA*=4 **deg.**
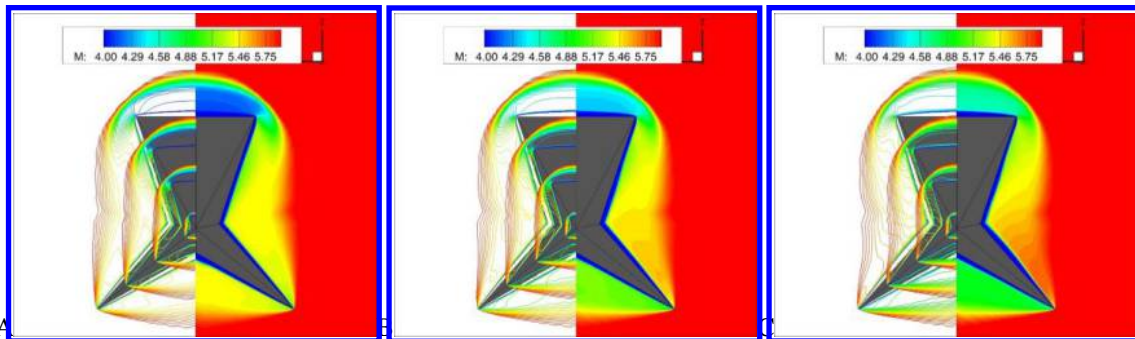

Figure 11. Mach number contours of the forebody (front view) with 100 deg rotation angle. (A) *AoA*=0 **deg. (B)** *AoA*=2 **deg. (C)** *AoA*=4 **deg.**
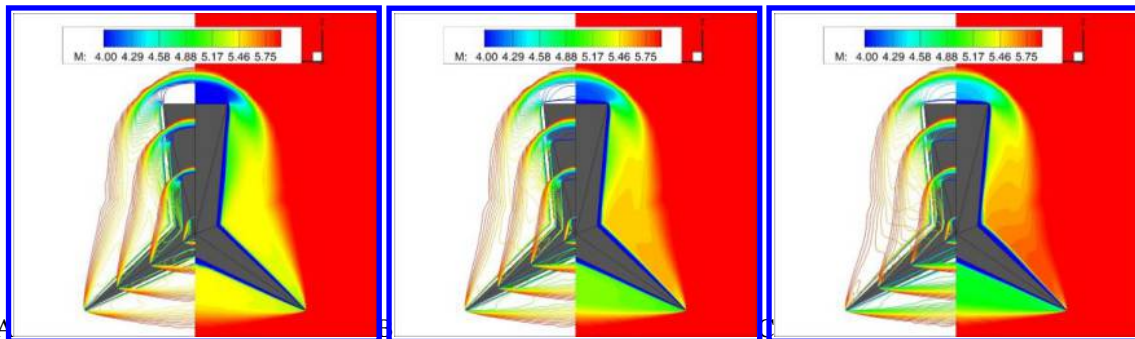

Figure 12. Mach number contours of the forebody (front view) with 110 deg rotation angle. (A) *AoA*=0 **deg. (B)** *AoA*=2 **deg. (C)** *AoA*=4 **deg.**
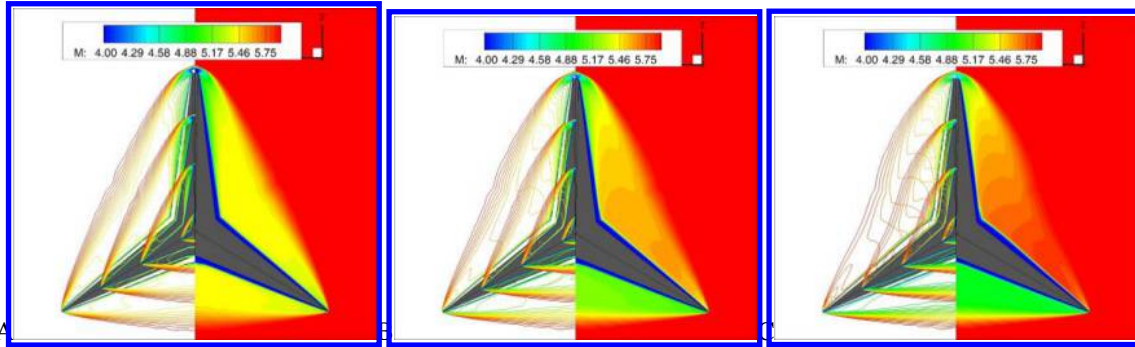
Figure 13. Mach number contours of the forebody (front view) with 120 deg rotation angle. (A) *AoA=0* **deg. (B)** *AoA=2 deg.* **(C)** *AoA=4 deg.*

case with 120 deg rotation angle. Even though the waverider characteristics is partially contaminated, as shown in each figure (A) in Fig.10 to Fig.13, the forebody still provides a uniformly distributed flow field at the outlet cross-section. Since the forebodies are generated at the same position of the conical flow field, the capture area of the forebodies is proportional to the mass flow. Thus, the greater the rotation angle, the more mass flow captured by the forebody. Furthermore, as shown in each right side of Fig.10 to Fig.13, the captured mass flow will be reduced at the lower side of the forebody as the angle of attack increases because that the compression of the free stream is weakened. Meanwhile, as the rotation angle of forebody increases, the reduction of the captured mass flow, which caused by the change of angle of attack, is more distinct. From the above, the trinal waveriders forebody could provide high quality flow field for the engine inlet. And forebodies with different rotation angle have their own advantages and disadvantages. Therefore, a rotation angle could be chosen by according to different requirements.

B. Aerodynamic Performance of the Preliminary Conceptual Configurations

The lift force matching the weight is an important consideration factor in flight. One of the effective ways to meet different weight requirements is that changing the aspect ratio of the vehicle. With the purpose of evaluating the aerodynamic performance of vehicles with different aspect ratio, as shown in Fig.14, four preliminary conceptual configurations are generated, which are owning aspect ratio of 0.8, 1.0, 1.2 and 1.4 respectively. In order to ensure the configurations are comparable, the bodies of four configurations are designed as the same profile. The length of the vehicles is set to 3 m. The length of the forebody is 1/6 of the vehicle length, and the rotation angle of the forebody selected as 110 deg. Because of the propulsion system design is not taken into account, an outlet is set at the end of the forebody. The boundary conditions of the free stream are set as a Mach number of 6, a flight
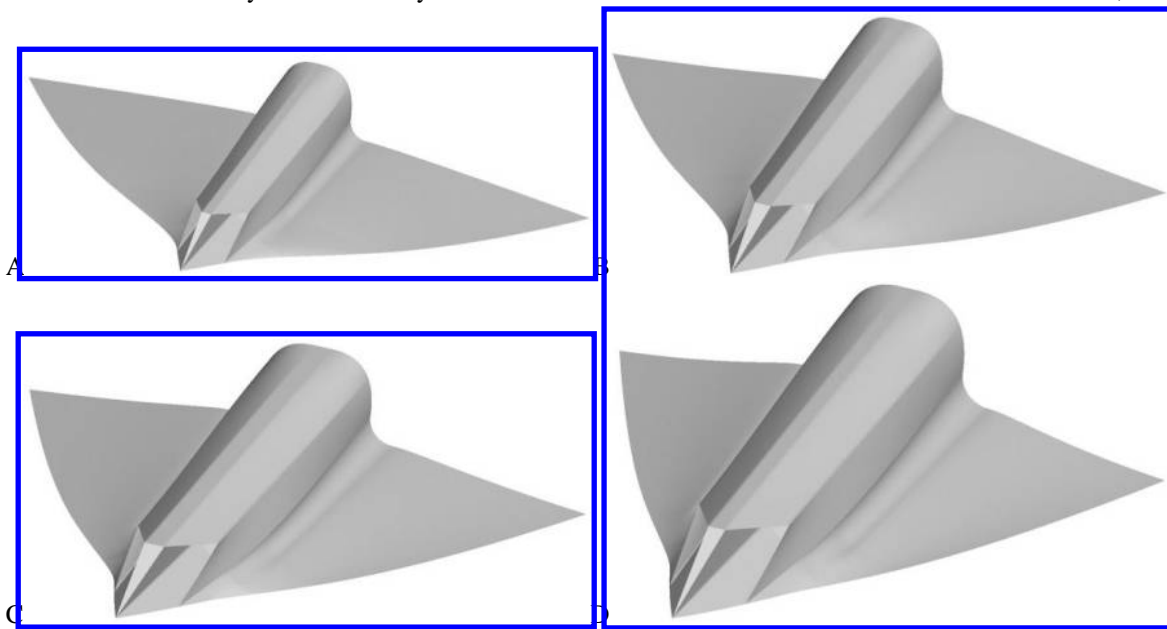

Figure 14. Preliminary conceptual configurations with different aspect ratio. (A) *L/W=0.8.* **(B)** *L/W=1.0.* **(C)** *L/W=1.2.* **(D)** *L/W=1.4.*

7

American Institute of Aeronautics and Astronautics

altitude of 30 km, a static pressure of 1196.983 Pa and a static temperature of 226.65 K. The angle of attack range from -4 deg to 4 deg, increments of 1 deg, and range from 4 deg to 10 deg, increments of 2 deg. Unstructured grid is adopted, as shown in Fig.15. The Euler equations are employed to evaluate the inviscid aerodynamic performance. The viscous drag force can be obtained by using the reference temperature method[24].

The pressure contour at the tail cross-section of the configuration, whose aspect ratio is 1.0, of AoA=0 deg is shown in Fig.16. It can be seen that the shock wave is fully attached to the leading edge of the lower surface. Other configurations have the same behavior. That means such configurations can give full play to the characteristics of waverider. The data of aerodynamic performance of preliminary conceptual configurations is shown in Fig.17. It illustrates that the four configurations have the same lift and drag force coefficients, which implying that the pressure on the lower and upper surfaces are evenly distributed. That phenomenon will provide a greater margin for the design of lift force matching the weight. Furthermore, the results in Fig.17 (C) indicate that the maximum L/D of configurations, of which the base drag is taken into account, is greater than
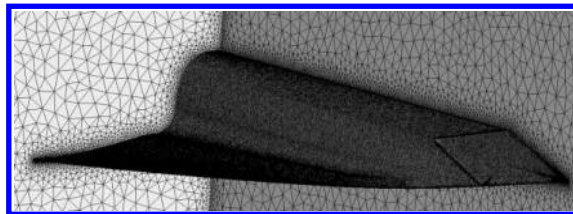

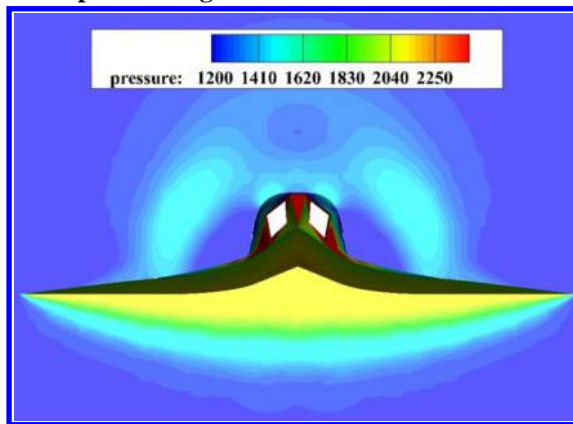**Figure 15. Unstructured gird of the preliminary conceptual configurations**

Figure 16. Pressure contour of the configuration of L/W=1.0 of AoA=0 deg (front view).
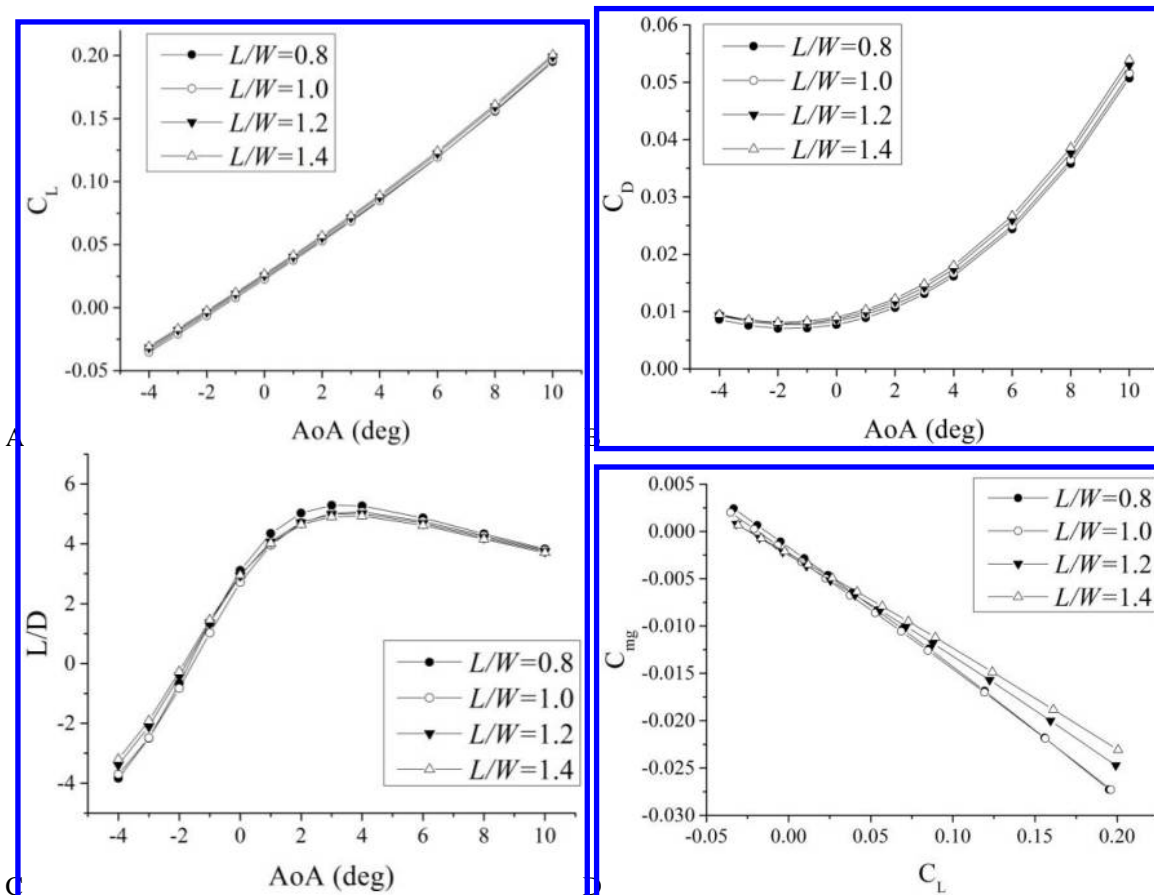

Figure 17. The aerodynamic performance data of preliminary conceptual configurations. (A) Lift force coefficient. (B) Drag force coefficient. (C) Lift to drag ratio. (D) Pitching moment coefficient.

8

American Institute of Aeronautics and Astronautics

5 in viscous condition. The maximum *L/D* is 5.285, when *AoA*=3 deg. And the *L/D* is relative higher in the *AoA*=1 to 5 deg, which is favorable flight conditions for the forebody operating. In addition, as shown in Fig.17 (D), by setting the centroid position at 0.57 of the vehicle length, the derivatives of the pitching moment coefficient to the lift force coefficient are less than zero. This manifested that such configurations are statically stable. In summary, the preliminary conceptual configurations achieve an aerodynamic performance.

V. Conclusion

In this paper, the splicing waverider generating method is developed. And the trinal waveriders forebody is generated by using a forebody design methodology which by rotating and assembling two waverider-based-surfaces. Finally, a family of novel waverider-based configurations, which integrate two dorsal mounted engines, is proposed. The results of forebodies analysis showed that a favorable quality of the flow field at the outlet cross-section could be assured. And the rotation angle of forebody could be chosen by according to different requirements. The results of the preliminary conceptual configurations illustrated that the maximum *L/D* of configurations is greater than 5 in viscous condition. And the *L/D* is relative higher in the *AoA*=1 to 5 deg, which is favorable flight conditions for the forebody operating.

Acknowledgments

References

[1]Joseph, M.H., James, S.M., Richard, C.M., "The X-51A Scramjet Engine Flight Demonstration Program," AIAA Paper 2008-2540.

[2]"High Speed Strike Weapon (HSSW) Demonstration Program." Department of the Air Force, https://www.fbo.gov/index?s=opportunity&mode=form&id=af217f963d28a50ef03f68c11f4e60a6&tab=core&_cview=1, 2012.

[3]"Meet the SR-72." http://www.lockheedmartin.com/us/news/features/2013/sr-72.html, 2013.

[4]Steven, W., Ming, T., Sue, M., and Caesar, M. "Falcon HTV-3X - A Reusable Hypersonic Test Bed," AIAA Paper 2008-2544.

[5]Langener, T., Steelant, J., Roncioni, P., Natale, P., and Marini, M. "Preliminary Performance Analysis of the LAPCAT-MR2 by means of Nose-to-Tail Computations," AIAA Paper 2012-5872, 2012.

[6]Giuseppe, P., Marco, M., Marco, C., Antonio, V., Tobias, L., and Johan, S. "Aerodynamic Characterization of HEXAFLY Scramjet Propelled Hypersonic Vehicle," AIAA Paper 2014-2844.

[7]Steelant, J., Langener, T., Matteo, F. D., et al., "Conceptual Design of the High-Speed Propelled Experimental Flight Test Vehicle HEXAFLY," AIAA Paper 2015-3539.

[8]Ferguson, F., Dasque, N., Dhanasar, M., et al., "Waverider design and analysis," AIAA Paper 2015-3508.

[9]Kuchemann D. *The Aerodynamic Design of Aircraft.* Oxford: Pergamon Press, 1978.

[10]Lobbia, M., Suzuki, K., "Multidisciplinary Design Optimization of Hypersonic Transport Configurations using Waveriders," AIAA Paper 2014-2359.

[11]Ding, F., Liu, J., Shen, C. B., et al, "Novel inlet-airframe integration methodology for hypersonic waverider vehicles," *Acta Astronautica*, Vol. 111, 2015, pp. 178-197.

[12]Yiqing, L., Ping, A., Chengjian, P., Rongqian, C., and Yancheng, Y. "Integration methodology for waverider-derived hypersonic inlet and vehicle forebody," AIAA Paper 2014-3229.

[13]Blankson, I. M. "Air-Breathing Hypersonic Cruise - Prospects for Mach 4-7 Waverider Aircraft," Journal of Engineering for Gas Turbines and Power-Transactions of the Asme Vol. 116, No. 1, 1994, pp. 104-115.

[14]Javaid, K. H., and Serghides, V. C. "Airframe-propulsion integration methodology for waverider-derived hypersonic cruise aircraft design concepts," Journal of Spacecraft and Rockets Vol. 42, No. 4, 2005, pp. 663-671.

[15]O'Neill, M. K. L., and Lewis, M. J. "Design Tradeoffs on Scramjet Engine Integrated Hypersonic Waverider Vehicles," Journal of Aircraft Vol. 30, No. 6, 1993, pp. 943-952.

[16]O'Neill, M. K. L., and Lewis, M. J. "Optimized Scramjet Integration on a Waverider," Journal of Aircraft Vol. 29, No. 6, 1992, pp. 1114-1121.

[17]Takashima, N., and Lewis, M. J. "Optimization of Waverider-Based Hypersonic Cruise Vehicles with Off-Design Considerations," Journal of Aircraft Vol. 36, No. 1, 1999, pp. 235-245.

[18]Mehta, U. B. "Strategy for developing air-breathing aerospace planes," Journal of Aircraft Vol. 33, No. 2, 1996, pp. 377-385.

[19]Bowcutt, K. G., Anderson, J. D., Capriotti, D., "Viscous Optimized Hypersonic Waveriders," AIAA Paper 1987-0272.

[20]Steven, W., and Frederick, R. "Falcon Hypersonic Technology Overview," AIAA Paper 2005-3253.

[21]Cui, K., Hu, S., Li, G., Qu, Z., and Situ, M. "Conceptual design and aerodynamic evaluation of hypersonic airplane with double flanking air inlets," Science China Technological Sciences Vol. 56, No. 8, 2013, pp. 1980-1988.

[22]Bowcutt, K. G., Smith, T. R., et al., "The Hypersonic Space and Global Transportation System: A Concept for Routine and Affordable Access to Space," AIAA Paper 2011-2295.

[23]Li, SX. *The Flow Characteristics for the Typical Model in Hypersonic Flows*. National Defense Industry Press, 2007.

[24]Anderson JD. *Hypersonic and high-temperature gas dynamics*. American Institute of Aeronautics and Astronautics, 2006.